Journal of Health Care and Research
(ISSN: 2582-8967)
Original Article
DOI: https://doi.org/10.36502/2025/hcr.6249

Identification of Shared Genes and Functional Pathways Between Skin Cancer and Skin Aging Based on Integrated Bioinformatic Analyses

Xingyu Chen[1], Xiaoyi Li[2]*
[1]International Curriculum Center, The High School Affiliated to Remin University of China, Beijing, P.R. China
[2]Department of Epidemiology and Health Statistics, School of Public Health, Peking University, Beijing, China

Corresponding Author: **Xiaoyi Li**
Address: Department of Epidemiology and Health Statistics, School of public health, Peking University, No.38 Road, Haidian District, Beijing, 100191, China; Tel: +86 18910306260; Email: sherryli@bjmu.edu.cn
Received date: 11 March 2025; **Accepted date**: 02 October 2025; **Published date**: 09 October 2025

Citation: Chen X, Li X. Identification of Shared Genes and Functional Pathways Between Skin Cancer and Skin Aging Based on Integrated Bioinformatic Analyses. J Health Care and Research. 2025 Oct 09;6(3):55-68.

Abstract

Backgrounds: Skin cancer (SC) and skin aging (SA) are polygenic phenotypes posing significant health risks. While molecular biomarkers and related pathways for each have been studied separately, shared mechanisms remain unclear. This study aimed to identify shared biomarkers and mechanisms between SC and SA using gene expression profiling, offering new insights for future research. This study identified shared differentially expressed genes (DEGs) of the two phenotypes, their related important pathways, and interactions between significant functional proteins.

Method: DEGs of SA and SC were identified via LIMMA analysis based on mRNA datasets from the Gene Expression Omnibus and ArrayExpress databases. Pathway enrichment analysis was conducted using the overrepresentation method to identify shared DEGs-associated KEGG pathways and GO terms. Using Cytoscape, protein-protein interaction (PPI) networks were constructed based on the STRING database. Core networks and top functional genes were identified using the MCODE plugin and CytoHubba plugin.

Results: Results showed SPRR1A and S100A2 as significant shared DEGs (GSE85358: P_{SPRR1A}=0.0028, $logFC_{SPRR1A}$ =-0.93; P_{S100A2}=0.0086, $logFC_{S100A2}$=-0.60; GSE2503: P_{SPRR1A}=0.0089, $logFC_{SPRR1A}$=2.5; P_{S100A2}=1.5, $logFC_{S100A2}$=0.0095; GSE3189: P_{SPRR1A} =1.7E-07, $logFC_{SPRR1A}$ =-3.4; P_{S100A2}=1.0E-14, $logFC_{S100A2}$=-4.5). Those shared genes enriched in immune response, endothelial cell migration, cellular process, and peptide cross-linking. In PPI analysis, top hub genes of networks were *PIK3R1, NANOG, VAV3, SMTN, SPRR1B, MET, MYLK, EPCAM, SPRR1A,* and *GATA3*.

Conclusions: Our findings elucidate shared genetic architectures between SC and SA. The identification of shared genes and protein-protein interaction networks associated with both SA and SC suggests an underlying molecular genetic mechanism, offering opportunities to develop therapeutic strategies against SA and SC comorbidity.

Keywords

Skin Aging, Melanoma, Non-Melanoma Skin Cancer, Biomarker

Abbreviations

NMSC: Nonmelanoma Skin Cancer; Including Squamous Cell Carcinoma; MSC: Melanoma Skin Cancer; GPL17077: Agilent-039494 Sureprint G3 Human GE V2 8x60k Microarray 039381; GPL96: Affymetrix Human Genome U133A Ar-Ray

Introduction

Skin cancer (SC), also referred to as cutaneous cancer, remains a growing global burden, accounting for around 30% of all cancer diagnoses worldwide in recent years [1]. SC is divided into melanoma (MSC) and non-melanoma (NMSC) skin cancer, with NMSC predominating; the most common types are basal cell carcinoma (BCC) and squamous cell carcinoma (SCC) [2]. Incidence, prevalence, and the types of SC vary greatly among populations and geographical locations. For instance, newly diagnosed MSC had a higher incidence among non-Hispanic White patients (26 per 100,000 individuals) compared to Native Americans/Alaskan Natives (7.4), Hispanics (4.6), Asians (1.3), and non-Hispanic Blacks (1.0). Some subtypes of NMSC, including Merkel cell carcinoma, occur more commonly in White patients compared with all non-White patients, making up about 4% of cases [3,4]. MSC is more invasive and aggressive than NMSC, accounting for about 80% of overall SC deaths [5]. Surgery, chemotherapy, and radiation therapy are the primary treatments for SC so far, but none of them can completely cure this disease and all have several negative consequences [6]. Due to cancer tolerance, poor bioavailability, and toxicity, these treatments cannot ensure that cancer cells are thoroughly eliminated and may even cause harsh side effects by damaging healthy cells [6-8]. Immunotherapy and targeted therapy, including immune checkpoint inhibitors and inhibitors targeting driver gene mutations, have significantly decreased recurrence and prolonged survival for some individuals with SC [7,9,10]. However, intrinsic and acquired resistance persist during SC therapy, underscoring the necessity for more robust diagnostic and predictive biomarkers, which would benefit the development of innovative therapeutic strategies.

Aging is an important risk factor for SC. According to the World Health Organization, the number and proportion of people aged 60 years and older in the population are constantly increasing [11]. MSC incidence markedly increased in persons aged 40 years and older from 2006 to 2015, in contrast to the reported observations in young adult populations in the United States [12]. Skin aging (SA) is characterized by age-related changes in the epidermis, dermis, and dermo-epidermal junction, and it can be classified into intrinsic aging and extrinsic aging [13]. Intrinsic skin aging occurs naturally via reductions in dermal mast cells, fibroblasts, and collagen production, while extrinsic skin aging mainly results from UV exposure, contributing to “photoaging” [13,14]. Since most functions in the human body are conducted by proteins, it has been hypothesized that SA might be associated with dysregulation of proteostasis or age-associated DNA damage, leading to the accumulation of unreplaced proteins [15,16].

Previous research suggests shared biological mechanisms between SC and SA. Firstly, UV irradiation, both natural and artificial, is considered the main driving factor in both photoaging and SC [17]. Sunburn and sun protection have been associated with the development of both MSC and NMSC [18,19], while lifetime sun exposure is considered the most important causative factor for actinic keratosis and lentigo maligna melanoma [18]. The oxidative stress pathway in the skin, resulting from UV light exposure, leads to abnormal reactive oxygen species accumulation, which may contribute to SA and SC occurrence [17,20,21]. In addition, aging can cause immune deficiency in the skin due to functional aging of the immune system, a process known as ‘immunosenescence’, and chronic low-grade inflammation, termed ‘inflammaging’, a continuous non-resolving immune response [22-24]. In cancer cases, mechanisms such as the age-induced increase in Treg (immunosuppressive T regulatory cells) may facilitate immune surveillance escape, contributing to the further development of SC; individuals taking immunosuppressive drugs are more susceptible to SC [24-26]. The mechanisms of SC or SA have been studied; however, the shared mechanisms between the two phenotypes remain to be elucidated. Understanding the shared pathogenic processes and the hub genes that control or regulate SC and SA may have far-reaching utility. It could facilitate efforts to identify novel

biomarkers for targeted therapy strategies, potentially delaying or halting the progression of both phenotypes simultaneously.

In the present study, an integrated bioinformatics analysis was performed to identify differentially expressed genes (DEGs) and hub genes and to examine their protein–protein interaction (PPI) networks and functional annotations. Briefly, the Gene Expression Omnibus (GEO) and ArrayExpress databases were used to obtain raw mRNA datasets. Through gene expression analysis, we identified DEGs shared between SC and skin aging. Gene Ontology (GO) and Kyoto Encyclopedia of Genes and Genomes (KEGG) pathway analyses were then conducted to determine the relevant pathways for these shared genes [27,28]. Further, tissue-specific gene enrichment analyses were performed to explore the association between DEGs and skin-specific biological functions, providing further evidence of their potential as biomarkers for both SA and SC. Using the database tool for the Retrieval of Interacting Genes/Proteins (STRING), PPI networks were constructed to identify hub genes and elucidate the interplay among the DEGs. This study provides better insight into the potential molecular mechanisms underlying SC and SA and explores novel preventive and therapeutic strategies.

Materials and Methods

Data Acquisition:

The gene expression profiles related to SC and SA were obtained from the Gene Expression Omnibus (GEO) database of the National Center for Biotechnology Information (NCBI) (https://www.ncbi.nlm.nih.gov/geo/). The retrieval formula was as follows: (non-melanoma [All Fields] OR melanoma [All Fields]) AND "Homo sapiens" [porgn] AND ("Expression profiling by array" [Filter] AND ("0001/01/01" [PDAT]: "2024/09/10" [PDAT])). All data collected were from the Caucasian population. Details of these datasets and their processing were provided in previous publications, as summarized in **Table-1**.

Quality Control for Gene Expression Data:

Quality control (QC) was performed on read count data. Prior to formal analysis, low-expression genes were filtered using the edgeR (v3.40.2) filterByExpr function, retaining genes with counts per million (CPM) ≥10 in at least 50% of individuals [29]. Normalization of count data was performed using the trimmed mean of M-values (TMM) method to correct for compositional biases. The limma-voom function was then applied: the voom transformation converted count data into log2 counts per million (log2-CPM) with precision weights, addressing heteroscedasticity and enabling linear modeling [30].

Identification of Shared DEGs:

Differential gene expression analysis was conducted using R software (v4.3.1) and the limma package (v3.58.1) to identify DEGs associated with SC or SA. LIMMA (Linear Models for Microarray) employs an empirical Bayes framework to enhance the statistical power of differential expression analysis by borrowing information across genes and using moderated t-tests and F-tests, where gene-specific variances are shrunk toward a common prior distribution [31]. The method constructs a linear model for each gene, incorporating experimental design factors (e.g., case-control group) through a design matrix, while empirical Bayes moderation adjusts the variance components in high-dimensional genomic data [31]. DEGs are displayed as volcano plots.

Table-1: Description of Gene Expression datasets(mRNA)

Phenotype	Source ID	Platform	Population	Tissue	Case	Controls
Skin Aging (SA)	GSE85358 [70]	GPL17077	European	Epidermis	24 Old	24 Young
Skin Cancer(SC)	GSE2503 [71]	GPL96	European	Skin	5 NMSC	6 Normal
	GSE3189 [72]	GPL96	America	Skin	45 MSC	18 Nevi + 7 Normal

Note: This table shows the source and the detailed information of every data sets. The source population, the sample tissue selec-tion, and the specific settings of its experimental groups and control groups are shown. The following experimental data are all based on Discovery groups.

The false positive rate was controlled by utilizing the Benjamini-Hochberg false discovery rate method to adjust the P values. An adjusted P value <0.01 and log2-fold change (logFC) ≥ 0.5 were set as cutoff criteria when the study used a case-control design. If logFC ≥ 0.5, the genes were considered upregulated in the disease group, and if logFC ≤ −0.5 (equivalent to |Fold Change| > 1.4), the genes were considered downregulated. Shared DEGs were defined as those significant in both SA and SC (MSC and NMSC). A Venn diagram was constructed using the ggvenn R package (v0.1.10) to compare and analyze the gene expression results, showing the number of DEGs shared between the two phenotypes and those associated with only one [32].

Functions and Pathways of Shared DEGs:

To distinguish and enrich the biological attributes—such as biological processes, cellular components, molecular functions, and pathways—of DEGs shared between SA and SC, as well as those associated with only one phenotype, functional enrichment analyses through GO and KEGG pathway analysis were carried out [27,28,33]. Utilizing the R package clusterProfiler (v4.4), enriched pathways and GO terms were tested for overrepresentation using the hypergeometric distribution.

Tissue-specific gene enrichment analyses were performed using the R package TissueEnrich (version 1.22.0) to investigate whether any DEGs showed significant enrichment in skin tissue (tissue-specific genes), providing further evidence of their potential as biomarkers for both SA and SC [34]. During the tissue-specific enrichment analysis, mRNA expression data from the Genotype-Tissue Expression (GTEx) database across 29 tissue types, including skin tissue, were used for evaluation [35]. For GO terms, KEGG pathways, and tissue enrichment, the Benjamini-Hochberg method was applied to adjust the p-values, with an adjusted p-value < 0.05 considered statistically significant [36,37].

PPI Network Construction and Screening of Hub Proteins:

The functional associations between gene-encoding proteins can provide insights into the potential functions of DEGs. The STRING (v12.0) biological database (https://string-db.org/, accessed on 2 Aug 2025) predicts the functional interactions of proteins by providing an association score, also called a combined score, based on seven distinct evidence channels [38,39]. Node pairs with an association score ≥ 0.4 (combined score) were selected for further analysis.

General PPI networks were then constructed using Cytoscape (version 3.10.1), with unconnected proteins hidden [40]. Key functional modules of proteins in the networks were identified using the molecular complex detection (MCODE) plugin of Cytoscape [41]. The parameters for MCODE analysis were set as follows: degree cutoff = 2, node score cutoff = 0.2, k-score = 2, and max depth = 100.

In addition, the CytoHubba plugin of Cytoscape was used to assess the top 10 DEGs using multiple algorithms: Maximal Clique Centrality (MCC), Density of Maximum Neighborhood Component (DMNC), Maximum Neighborhood Component (MNC), Degree, Edge Percolated Component (EPC), Bottleneck, Eccentricity, Closeness, and Radiality [42].

Results

Differential Expression Analysis Suggests Substantial Genes as Shared Signal Mediators in Both SA and SC:

Based on these mapped reads, we quantified the expression levels of 16000～25000 genes. To identify shared signatures between SA and SC across different populations or different skin tissues, differential expression analyses were performed in 1 SA mRNA-level gene expression dataset and 2 SC mRNA-level gene expression datasets previously collected from the GEO database, respectively. We found substantial differences between old and middle-aged or young samples (**Fig-1A**). The limma analyses of the mRNA expression signatures from GSE85358 revealed 669 differentially expressed genes (DEGs) (p value <0.01 and |logFC| ≥ 0.5) in epidermal tissue between old and young individuals, 418 of them remain after Benjamini–Hochberg correction (adjusted p value <0.01). GSE2503 and GSE3189, which represent the different types of SC, were also used to perform limma analyses. Using linear regression models, 26 showed significant differences between NMSC and normal tissue (944 when in

unadjusted condition) in GSE2503, while GSE3189 contained 4303 DEGs (4473 when in unadjusted condition).

Among these DEGs, 2 and 98 overlapped in GSE85358 and GSE2503 or GSE3189 respectively (Supplementary material description: **Suppl. Table-S1** and **Suppl. Table-S2**). Among these overlapping DEGs, *SPRR1A* and *S100A2* which are well recognized as shared genes both in two pairs of SA and SC, were shown in the center of the Venn plot (**Fig-1B**). The expression of *SPRR1A* and *S100A2* of samples across different phenotypes was detected and plotted with a box diagram (**Fig-1C**). The result of genes *SPRR1A* and *S100A2* expression can contribute to differentiating the properties of SA and SC. Interestingly, the directions of correlation between SA and NMSC or MSC are visually different, suggesting the distinct pathophysiological mechanisms in the two types of SC.

As **Fig-1A** shows, three sets of volcano plots are roughly symmetrical, thus it can be inferred that there is no significant difference in the absolute value of effect size, the significance of gene expression, and the quantity of up-regulated and down-regulated genes in either SA or SC groups. Besides, both two SC groups have a wider range of effect size, forming an obvious contrast with the SA group. The effect size of SC groups is located between -6 and 6 in general, but in the SA group, this value is only between -1.5 and 1.5, which means more SC DEGs are relatively effective. Focusing on the comparison of the significance level of DEGs, it is clear that MSC and SA have higher expression significance and the expression difference compared NMSC and normal tissue is not marked.

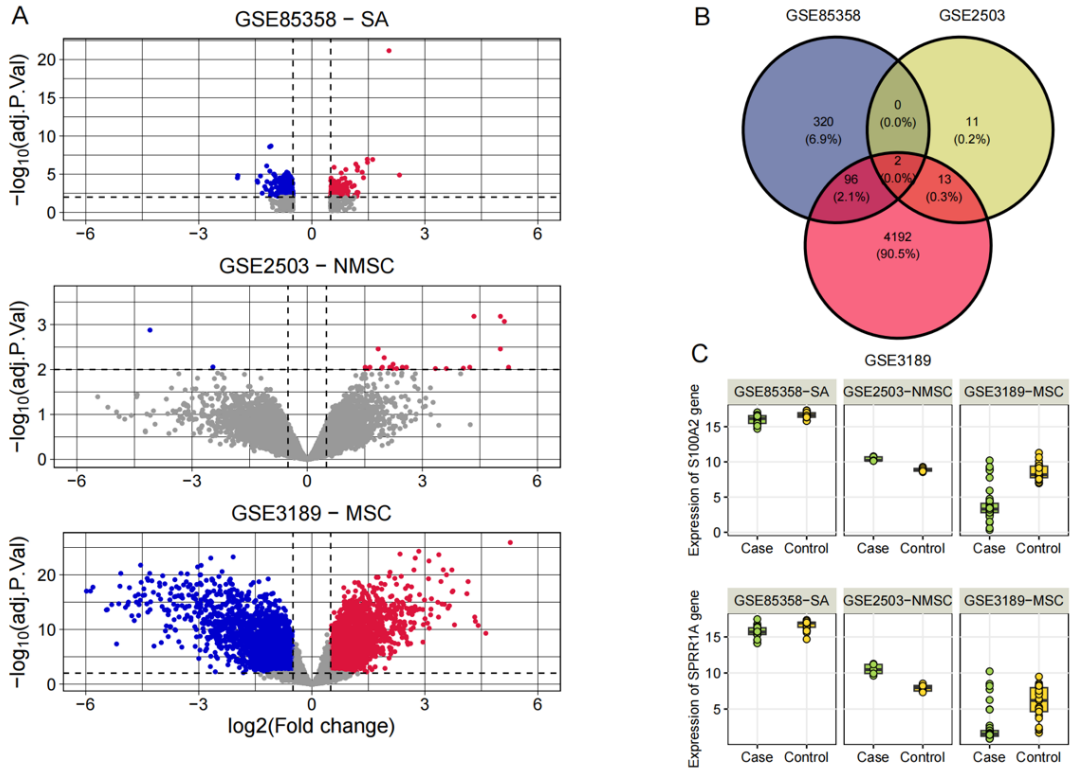

Fig-1: Differential Expression Analysis Suggests Substantial Genes

A: Volcano Plot: The horizontal axis value LogFC is used to express the effect value of a gene for a disease, i.e., its risk coefficient, and the vertical axis value adjust P value is used to express the significance of gene. The critical criteria for determining whether a gene is significant or not are indicated by the dotted line, with gray points being ineligible genes and points with color indicating significant genes. Blue dots are down-regulated expressed significant genes and red dots are up-regulated expressed significant genes;

B: Venn Plot: Summarizing the intersecting significant DEGs for MSC, NMSC, and SA (shared DEG)

C: Box Plot: Showing the expression distribution of two intersecting significant DEGs that result from Venn plot in the three disease datasets.

Despite NMSC and MSC both belonging to SC, there are several differences between their results—remarkable discrepancy in the number of DEGs, DEG quantity difference between the unadjusted and adjusted condition, and the number of shared DEGs with the SA group. MSC has a much larger number than NMSC in both DEG number and SA shared DEG number, and most DEGs of NMSC are excluded after the Benjamini–Hochberg (BH) correction.

According to the pie graph (**Fig-1B**), 98 DEGs are shared by MSC and SA, far more than the number of DEGs shared by NMSC and MSC or SA. Interestingly, this could imply that the molecular mechanism between MSC and SA seems to be closely related, and even have a tighter connection than the two subtypes of SC.

Functional Enrichment and Tissue-Specific Enrichment Analysis of the DEGs Shared with SA and SC:

To gain a more comprehensive understanding of the selected DEGs, GO function and KEGG pathway enrichment analyses were performed. For the shared genes identified in the SA and NMSC pair, GO analysis identified 14 enriched GO terms, indicating that the DEGs were predominantly associated with the following functions: cell differentiation, epithelial cell and tissue migration, peptide cross-linking, calcium-dependent protein binding, and skin development. No KEGG pathway was identified (**Table-2**).

Table-2: GO and KEGG results of shared gene sets between SA and SC

Trait Pair	ID	Description	GR	P	P.adj	Gene name
SA and NMSC	GO:0018149	peptide cross-linking	01-Feb	2.97E-03	3.26E-02	SPRR1A
	GO:0031424	Keratinization	01-Feb	8.78E-03	4.44E-02	SPRR1A
	GO:0030216	keratinocyte differentiation	01-Feb	1.87E-02	4.44E-02	SPRR1A
	GO:0009913	epidermal cell differentiation	01-Feb	2.58E-02	4.44E-02	SPRR1A
	GO:0043542	endothelial cell migration	01-Feb	2.99E-02	4.44E-02	S100A2
	GO:0043588	skin development	01-Feb	3.33E-02	4.44E-02	SPRR1A
	GO:0010631	epithelial cell migration	01-Feb	3.90E-02	4.44E-02	S100A2
	GO:0090132	epithelium migration	01-Feb	3.94E-02	4.44E-02	S100A2
	GO:0090130	tissue migration	01-Feb	3.99E-02	4.44E-02	S100A2
	GO:0008544	epidermis development	01-Feb	4.04E-02	4.44E-02	SPRR1A
	GO:0001667	ameboidal-type cell migration	01-Feb	4.99E-02	4.99E-02	S100A2
	GO:0001533	cornified envelope	01-Feb	6.03E-03	6.03E-03	SPRR1A
	GO:0030280	structural constituent of skin epidermis	01-Feb	3.89E-03	7.78E-03	SPRR1A
	GO:0048306	calcium-dependent protein binding	01-Feb	8.52E-03	8.52E-03	S100A2
SA and MSC	GO:0002429	Immune response-activating cell surface receptor signaling pathway	Sep-96	3.51E-05	4.12E-02	NINJ1/BLNK/RFTN1/GATA3/VAV3/SHB/PIK3R1/GPLD1/TLR5
	GO:0010595	positive regulation of endothelial cell migration	Jun-96	5.32E-05	4.12E-02	ANXA3/MET/RIN2/GATA3/EDN1/GPLD1
	GO:0002768	immune response-regulating cell surface receptor signaling pathway	Sep-96	6.74E-05	4.12E-02	NINJ1/BLNK/RFTN1/GATA3/VAV3/SHB/PIK3R1/GPLD1/TLR5
	GO:0043542	endothelial cell migration	Aug-96	1.01E-04	4.61E-02	ANXA3/ID1/MET/RIN2/GATA3/EDN1/S100A2/GPLD1
	GO:0003779	actin binding	Sep-96	4.53E-04	4.67E-02	MYLK/ACTN1/CNN1/SMTN/MYO10/DST/TPM4/PHACTR4/ALKBH4
	GO:0048306	calcium-dependent protein binding	Apr-96	7.60E-04	4.79E-02	S100A6/ANXA3/RAC3/S100A2
	GO:0070851	growth factor receptor binding	May-96	7.63E-04	4.99E-02	GATA3/VAV3/IL6R/FLRT3/TLR5
	hsa04510	Cellular Processes	Jul-45	6.56E-05	0.012	MYLK/ACTN1/COL9A1/MET/VAV3/RAC3/PIK3R1

Note: GR: Gene Ratio, genes of interest in the gene set / total genes of interest; P.adj: the adjusted P value according to the Benjamini and Hochberg correction.

For the shared genes identified in the SA and MSC pair, DEGs were significantly concentrated in specific functions according to GO analysis, including immune response–activating cell surface receptor signalling pathway, positive regulation of endothelial cell migration, immune response–regulating cell surface receptor signalling pathway, and endothelial cell migration (**Table-2**). KEGG analysis identified only one pathway as significantly enriched: Cellular Processes. These results suggest that the majority of the overlapping DEGs are related to cancer.

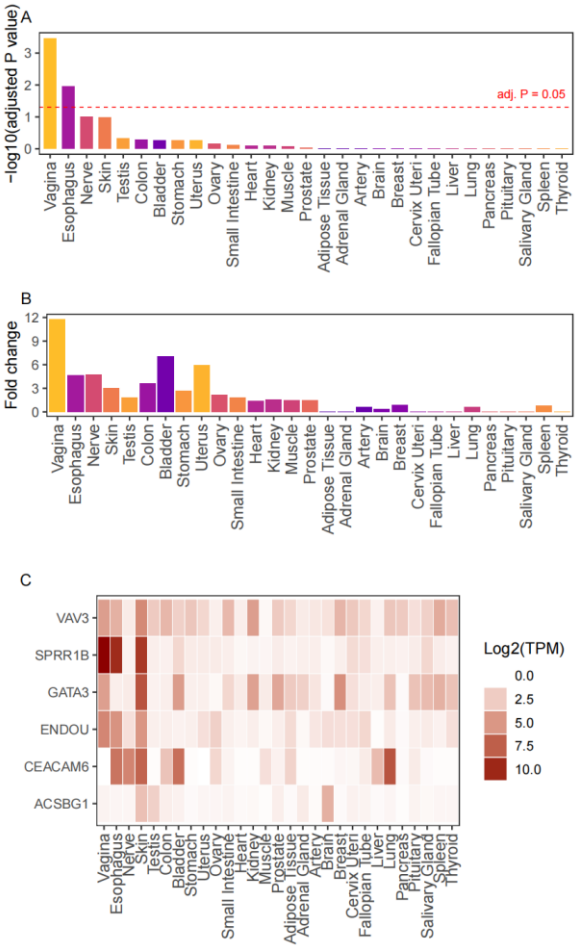

Fig-2: Tissue Enrichment Analysis Suggests Tissue-Specific Enriched Genes

A: Box plot of P values for identified DEGs in 29 tissues. Red line represents the threshold value of P value.

B: Box plot of fold changes for the identified DEGs in 29 tissues. Fold changes represent the ratio of the proportion of tissue-specific genes in the target gene set to the proportion of the same tissue-specific genes in the background genome, indicating the degree of enrichment of that tissue within the gene set.

C: Heatmap for 6 tissue-specific enriched genes identified in skin tissue.

Finally, tissue-specific enrichment analysis was performed for the shared DEGs (**Fig-2**). The results showed that skin tissue exhibited a 3.04-fold enrichment in our gene set compared to the background genome, indicating a suggestive association between the DEGs and skin-specific biological functions (Fold change = 3.04, P = 0.011, PBH = 0.10; **Fig-2a** and **Fig-2b**). In addition, six genes were identified with expression levels in 1 to 7 tissues that were at least five-fold higher than in all other tissues, specifically in skin tissue.

From Shared DEGs to PPI Network: Identification of Hub Genes:

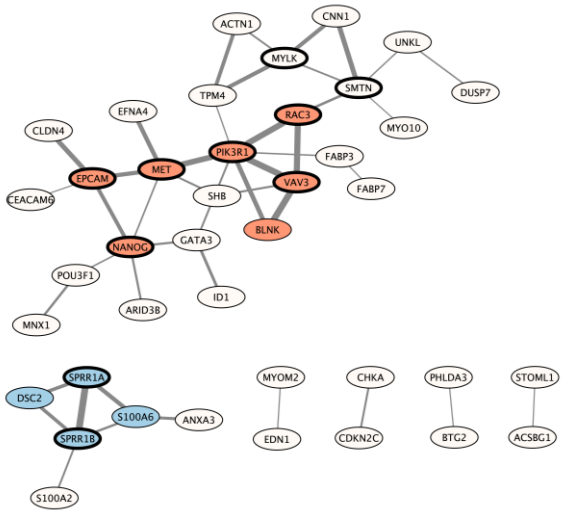

Fig-3: Network of SA and MSC pair

The thickness of gene connection lines indicates the degree of correlation of gene co-expression. The linked genes are related in expression and may belong to the same functional group. Apart from the light pink (which means not belonging to any network), different colors represent different functional subnetworks. Two individually paired genes are identified as highly related subnetworks.

The network of the shared DESs between SA and SC, obtained by analyzing our data, was primarily constructed based on the combined scores collected from the STRING database. We filtered the nodes and their edges with moderate confidence (combined score ≤ 0.4). For the SA and NMSC pair, no network and sub-network were identified, which may be because of not enough input genes (2 shared DEGs). For the SA and MSC pair, the final general network contains 40 nodes(genes) and 44 edges (combined score) (**Fig-3**), and 2 sub-networks scoring among 3 were identified. of 40 genes, some of the genes such as SPRR1A, *MET,*

VAV3, and *BLNK* are the core nodes of the subnetworks, suggesting the potential genetic factor of SA and MSC. Moreover, 9 methods including MCC, MCN, and degree were used to select the hub genes from the PPI network using the CytoHubba plugin with default parameters in Cytoscape. This process revealed top 10 hub genes, which are *PIK3R1, NANOG, VAV3, SMTN, SPRR1B, MET, MYLK, EPCAM, SPRR1A, RAC3* (**Table-3**).

Discussion

This study unveiled several genes that are significantly associated with both SC and SA, such as SPRR1A and S100A2. In functional enrichment analysis, the identified DEGs were significantly enriched in GO terms and pathways related to cell growth and development, cell/tissue migration, and immunity. Furthermore, the PPI network revealed co-expression relationships among the gene sets and highlighted the important roles of DEGs such as PIK3R1 and MET within their subnetworks. These results provide a theoretical basis for identifying the shared biological mechanisms of SA and SC.

Table-3: Top 10 genes in the network of shared DEGs between Skin Aging and MSC

Node Name	MCC	DMNC	MNC	Degree	EPC	BottleNeck	EcCentricity	Closeness	Radiality
PIK3R1	8	0.31	3	7	10.97	25	0.16	14.33	4.68
MET	5	0.31	2	5	9.95	7	0.13	12.95	4.52
SPRR1B	5	0.31	3	4	3.83	3	0.08	4.5	0.54
SMTN	5	0.31	2	5	8.48	5	0.11	11.38	4.11
VAV3	5	0.31	3	4	9.59	3	0.13	11.28	4.29
NANOG	5	0.31	2	5	9.34	4	0.11	11.93	4.24
SPRR1A	4	0.31	3	3	3.7	1	0.08	4	0.51
EPCAM	4	0.31	2	4	8.14	3	0.11	11.1	4.16
MYLK	4	0.31	2	4	8.05	1	0.11	10.47	4
RAC3	3	0.31	2	3	9.37	6	0.13	11.53	4.39

Potential Shared Biomarkers for Both Skin Aging and Skin Cancer:

SPRR1A and S100A2, shared DEGs of SA and both subtypes of SC, were downregulated in SA and MSC and upregulated in NMSC. SPRR1A, a human protein-coding gene, produces small proline-rich protein 1A, a structural component of the epidermis involved in keratinocyte differentiation and peptide cross-linking [43]. Previous studies have shown that SPRR1A is expressed at high basal levels in advanced stages of SC and is considered a marker of squamous epithelial differentiation and metastatic transformation of melanoma [44-46]. Conversely, other studies indicated that downregulated SPRR1A expression correlates with later cancer stages and decreased survival rates [47]. In this study, SPRR1A showed differential regulation, providing new evidence for understanding its role in MSC and NMSC.

The S100A2 gene encodes S100 Calcium Binding Protein A2, a protein localized to the cytoplasm and/or nucleus that regulates several cellular processes, including cell cycle progression and differentiation [48]. S100A2 has been considered a tumor suppressor gene in some studies, as it can enhance the transcriptional activity of p53 family members, and p53 mutation or degradation increases susceptibility to NMSC [49-51]. However, these findings do not fully align with our results, highlighting the complexity of S100A2-related mechanisms in SC.

Shared Mechanisms Between Skin Aging and Melanoma:

For SA and MSC, immune response–activating/regulating cell surface receptor signaling pathways were identified as relevant. The immune response–activating pathway involves the binding of extracellular ligands to cell surface receptors, triggering or sustaining an immune response [52]. The immune response–regulating pathway involves similar molecular interactions that modulate immune responses [53]. NINJ1 and BLNK are highly associated with these pathways. NINJ1 encodes a 16-kDa cell-surface protein with two transmembrane regions,

involved in inflammation, tumor suppression, and necrotic/apoptotic cell death [54]. BLNK encodes an adaptor molecule expressed in B cells [55]. Previous research shows that melanomas insufficiently responsive to immune checkpoint blockade often have gene losses linked to senescence and amplification of senescence inhibitors. Melanoma-associated fibroblasts can create an immunosuppressed microenvironment by upregulating inflammatory and immune-inhibitory factors [56], altering extracellular metabolites like lactate, glucose, and arginine to suppress immune cells or polarize them toward a pro-tumor phenotype. There are no existing studies discussing the role of these two immune response pathways and their most related DEGs in both SA and SC, suggesting that our results provide novel insight into their shared mechanisms.

Positive regulation of endothelial cell migration was also highly enriched in both SA and MSC. Chemotactic and mechanotactic signals guide endothelial cell migration, involving extracellular matrix degradation to support cell mobility [57]. Silencing ANXA3 inhibits growth and migration in certain cancer cells, highlighting its role in cellular growth regulation and signaling [58]. MET, a proto-oncogene, encodes a receptor tyrosine kinase linked to cell survival, embryonic development, and cell movement. Studies suggest aged skin may have a predisposition for tumor cell migration [59]. Senescent dermal fibroblasts release chemerin, which enhances squamous cell carcinoma migration via the MAPK pathway [60]. While prior studies on SC metastasis describe several pathways, regulation of endothelial cell migration has not been emphasized, nor have key functional genes overlapped with our findings. No SA study has specifically focused on endothelial cell migration.

KEGG analysis of SA and MSC revealed enrichment in cellular processes, including DEGs such as MYLK and ACTN1. MYLK encodes smooth muscle and non-muscle myosin light chain kinase isoforms, enzymes reliant on calcium and calmodulin that regulate contractility and telokin function, respectively [61]. ACTN1 encodes an F-actin cross-linking protein anchoring actin to intracellular structures [62]. Other reported SC biomarkers include PDGFR α/β, αSMA, fibronectin, COL11A1, FAP, tenascin-C, vimentin, FSP-1, and GFPT2 [63].

In the PPI network of shared DEGs for the SA–MSC pair, PIK3R1 and RAC3 were the top DEGs, suggesting potential biomarkers for both SA and MSC. PIK3R1 encodes the phosphoinositide-3-kinase regulatory subunit 1 [64], part of the PI3K–Akt–mTOR signaling pathway, which regulates senescence and self-renewal of skin cells, such as skin-derived precursors [65]. Activation of this pathway protects melanocytes from excessive oxidative stress, a key risk factor for SA and SC [66]. RAC3, a member of the RAS superfamily, encodes a GTPase that regulates cell growth, cytoskeleton remodeling, and protein kinase activity [67].

Shared Mechanisms Between Skin Aging and Non-Melanoma Skin Cancer:

For DEGs in SA and NMSC, peptide cross-linking was the most significantly enriched function. Peptide cross-linking involves covalent bond formation within or between peptide chains [68]. The associated DEG SPRR1A, a top gene shared between SC and SA, encodes a small proline-rich protein precursor of the keratinocyte cornified envelope, involved in peptide cross-linking, keratinocyte differentiation, and cross-bridging in stratified squamous epithelia [2,47,48]. DNA–protein cross-linking, a chemical bonding process between DNA and proteins, may affect peptide cross-linking and contributes to cancer and aging. This occurs when cellular DNA is exposed to agents such as reactive oxygen species, transition metals, and UV light, many of which are carcinogenic [69]. Studies on peptide cross-linking in SC and SA are limited; few bioinformatics studies mention it, and none have explored its significance in SA. This pathway may represent a novel shared functional mechanism of SA and NMSC.

Limitations

To our knowledge, this is the first study to explore shared genes and functional pathways in SC and SA. However, there are limitations. First, the sample size of mRNA data is relatively small, especially for NMSC, resulting in low statistical power. Second, the study is based on publicly available GEO data, which requires further experimental validation. Wet-lab studies (e.g., cell-based assays and transgenic mouse models) are needed to confirm the functional effects of the identified DEGs. Additionally, there is a lack of SA and SC data for

non-Caucasian populations. Differences in shared mechanisms across ethnic groups need further investigation, possibly limited by the small NMSC sample size used in this study.

Conclusions

This research used mRNA datasets from Caucasian populations to investigate shared biomarkers and mechanisms of SA and SC. Shared DEGs were identified, functional enrichment analyses were conducted, and biological protein–protein interaction (PPI) networks were constructed using STRING. This study identified SPRR1A and S100A2 as key genes, which may serve as potential shared biomarkers for SC and SA. Immune response and peptide cross-linking pathways were shown to play important roles in SC and SA, particularly in MSC. The pathways discovered in this study (immune response, endothelial cell migration, cellular processes, peptide cross-linking) have not been well explored in the SA and SC fields, indicating that our findings may provide new evidence for mechanistic research.

Significant differences between MSC and NMSC were observed, such as opposite directions of DEG regulation. These results highlight the complexity of SC mechanisms and the pleiotropic roles of significant DEGs. Overall, this study reveals a shared molecular framework between SC and SA, offering new insights for understanding the underlying molecular genetic mechanisms. However, further molecular epidemiological studies with larger sample sizes and experimental validations are needed to confirm the shared genes identified in this study.

Ethics Statement

Not applicable. All datasets used in the present study were approved by the ethics committees in the original studies. Informed consent was obtained from all participants. No additional institutional review board approval was required.

Supplementary Material Description

Appendices for **Suppl. Table-S1** and **Suppl. Table-S2** are provided in the supplementary material. **Suppl. Table-S1** lists the differentially expressed genes identified in both melanoma and skin aging (adjusted $P < 0.05$). **Suppl. Table-S2** lists the differentially expressed genes identified in both non-melanoma skin cancer and skin aging (adjusted $P < 0.05$).

Acknowledgement

We thank the data submitters and the developers of the GEO database, GO database, KEGG pathway database, and STRING database for making this study possible. We also acknowledge the developers of R software and the packages used in this study.

Funding Statement

This research did not receive any specific grant from funding agencies in the public, commercial, or not-for-profit sectors.

Conflict of Interest

The authors have read and approved the final version of the manuscript. The authors have no conflicts of interest to declare.

References

[1] Urban K, Mehrmal S, Uppal P, Giesey RL, Delost GR. The global burden of skin cancer: A longitudinal analysis from the Global Burden of Disease Study, 1990-2017. JAAD Int. 2021 Jan 4;2:98-108. [**PMID**: 34409358]

[2] Griffin LL, Ali FR, Lear JT. Non-melanoma skin cancer. Clin Med (Lond). 2016 Feb;16(1):62-65. [**PMID**: 26833519]

[3] Siegel RL, Miller KD, Jemal A. Cancer statistics, 2020. CA Cancer J Clin. 2020 Jan;70(1):7-30. [**PMID**: 31912902]

[4] Trofymenko O, Zeitouni NC, Kurtzman DJB. Factors associated with advanced-stage Merkel cell carcinoma at initial diagnosis and the use of radiation therapy: Results from the National Cancer Database. J Am Acad Dermatol. 2018 Oct;79(4):680-88. [**PMID**: 29574087]

[5] Jones OT, Ranmuthu CKI, Hall PN, Funston G, Walter FM. Recognising Skin Cancer in Primary Care. Adv Ther. 2020 Jan;37(1):603-16. [**PMID**: 31734824]

[6] Hasan N, Nadaf A, Imran M, Jiba U, Sheikh A, Almalki WH, Almujri SS, Mohammed YH, Kesharwani P, Ahmad FJ. Skin cancer: understanding the journey of transformation from conventional to advanced treatment approaches. Mol Cancer. 2023 Oct 6;22(1):168. [**PMID**: 37803407]

[7] Hasan N, Imran M, Sheikh A, Tiwari N, Jaimini A, Kesharwani P, Jain GK, Ahmad FJ. Advanced

multifunctional nano-lipid carrier loaded gel for targeted delivery of 5-flurouracil and cannabidiol against non-melanoma skin cancer. Environ Res. 2023 Sep 15;233:116454. [**PMID**: 37343751]

[8] Nurgali K, Jagoe RT, Abalo R. Editorial: Adverse Effects of Cancer Chemotherapy: Anything New to Improve Tolerance and Reduce Sequelae? Front Pharmacol. 2018 Mar 22;9:245. [**PMID**: 29623040]

[9] Kumari S, Choudhary PK, Shukla R, Sahebkar A, Kesharwani P. Recent advances in nanotechnology based combination drug therapy for skin cancer. J Biomater Sci Polym Ed. 2022 Aug;33(11):1435-68. [**PMID**: 35294334]

[10] Luke JJ, Flaherty KT, Ribas A, Long GV. Targeted agents and immunotherapies: optimizing outcomes in melanoma. Nat Rev Clin Oncol. 2017 Aug;14(8):463-82. [**PMID**: 28374786]

[11] World Health Organization. Ageing and health [Internet]. Geneva: WHO; 2024 [cited 2025 Jun 29]. Available from: https://www.who.int/news-room/fact-sheets/detail/ageing-and-health

[12] Paulson KG, Gupta D, Kim TS, Veatch JR, Byrd DR, Bhatia S, Wojcik K, Chapuis AG, Thompson JA, Madeleine MM, Gardner JM. Age-Specific Incidence of Melanoma in the United States. JAMA Dermatol. 2020 Jan 1;156(1):57-64. [**PMID**: 31721989]

[13] Zargaran D, Zoller F, Zargaran A, Weyrich T, Mosahebi A. Facial skin ageing: Key concepts and overview of processes. Int J Cosmet Sci. 2022 Aug;44(4):414-420. [**PMID**: 35426152]

[14] Sachs DL, Varani J, Chubb H, Fligiel SEG, Cui Y, Calderone K, Helfrich Y, Fisher GJ, Voorhees JJ. Atrophic and hypertrophic photoaging: Clinical, histologic, and molecular features of 2 distinct phenotypes of photoaged skin. J Am Acad Dermatol. 2019 Aug;81(2):480-88. [**PMID**: 30954583]

[15] Höhn A, Weber D, Jung T, Ott C, Hugo M, Kochlik B, Kehm R, König J, Grune T, Castro JP. Happily (n)ever after: Aging in the context of oxidative stress, proteostasis loss and cellular senescence. Redox Biol. 2017 Apr;11:482-501. [**PMID**: 28086196]

[16] Csekes E, Račková L. Skin Aging, Cellular Senescence and Natural Polyphenols. Int J Mol Sci. 2021 Nov 23;22(23):12641. [**PMID**: 34884444]

[17] Guida S, Pellacani G, Ciardo S, Longo C. Reflectance Confocal Microscopy of Aging Skin and Skin Cancer. Dermatol Pract Concept. 2021 May 20;11(3):e2021068. [**PMID**: 34123564]

[18] Kennedy C, Bajdik CD, Willemze R, De Gruijl FR, Bouwes Bavinck JN; Leiden Skin Cancer Study. The influence of painful sunburns and lifetime sun exposure on the risk of actinic keratoses, seborrheic warts, melanocytic nevi, atypical nevi, and skin cancer. J Invest Dermatol. 2003 Jun;120(6):1087-93. [**PMID**: 12787139]

[19] Iannacone MR, Hughes MC, Green AC. Effects of sunscreen on skin cancer and photoaging. Photodermatol Photoimmunol Photomed. 2014 Apr-Jun;30(2-3):55-61. [**PMID**: 24417448]

[20] Varga R, Gross J. Oxidative Stress Status and Its Relationship to Skin Aging. Plast Aesthet Nurs (Phila). 2023 Jul-Sep 01;43(3):141-48. [**PMID**: 37389631]

[21] Apalla Z, Nashan D, Weller RB, Castellsagué X. Skin Cancer: Epidemiology, Disease Burden, Pathophysiology, Diagnosis, and Therapeutic Approaches. Dermatol Ther (Heidelb). 2017 Jan;7(Suppl 1):5-19. [**PMID**: 28150105]

[22] Vukmanovic-Stejic M, Rustin MH, Nikolich-Zugich J, Akbar AN. Immune responses in the skin in old age. Curr Opin Immunol. 2011 Aug;23(4):525-31. [**PMID**: 21703840].

[23] Pająk J, Nowicka D, Szepietowski JC. Inflammaging and Immunosenescence as Part of Skin Aging-A Narrative Review. Int J Mol Sci. 2023 Apr 24;24(9):7784. [**PMID**: 37175491]

[24] Ruhland MK, Loza AJ, Capietto AH, Luo X, Knolhoff BL, Flanagan KC, Belt BA, Alspach E, Leahy K, Luo J, Schaffer A, Edwards JR, Longmore G, Faccio R, DeNardo DG, Stewart SA. Stromal senescence establishes an immunosuppressive microenvironment that drives tumorigenesis. Nat Commun. 2016 Jun 8;7:11762. [**PMID**: 27272654]

[25] Li X, Kostareli E, Suffner J, Garbi N, Hämmerling GJ. Efficient Treg depletion induces T-cell infiltration and rejection of large tumors. Eur J Immunol. 2010 Dec;40(12):3325-35. [**PMID**: 21072887]

[26] Kreher MA, Noland MMB, Konda S, Longo MI, Valdes-Rodriguez R. Risk of melanoma and nonmelanoma skin cancer with immunosuppressants, part I: Calcineurin inhibitors, thiopurines, IMDH inhibitors, mTOR inhibitors, and corticosteroids. J Am Acad Dermatol. 2023 Mar;88(3):521-30. [**PMID**: 36460257]

[27] Kanehisa M, Goto S. KEGG: kyoto encyclopedia of genes and genomes. Nucleic Acids Res. 2000 Jan 1;28(1):27-30. [**PMID**: 10592173]

[28] Thomas PD, Ebert D, Muruganujan A, Mushayahama T, Albou LP, Mi H. PANTHER: Making genome-scale phylogenetics accessible to all. Protein Sci. 2022 Jan;31(1):8-22. [**PMID**: 34717010]

[29] Chen Y, Chen L, Lun ATL, Baldoni PL, Smyth GK. edgeR v4: powerful differential analysis of sequencing data with expanded functionality and improved support for small counts and larger datasets. Nucleic Acids Res. 2025 Jan 11;53(2):gkaf018. [**PMID**: 39844453]

[30] Law CW, Chen Y, Shi W, Smyth GK. voom: Precision weights unlock linear model analysis tools for RNA-seq read counts. Genome Biol. 2014 Feb 3;15(2):R29. [**PMID**: 24485249]

[31] Smyth GK. Limma: linear models for microarray data. Bioinformatics and computational biology solutions using R and Bioconductor. Springer. 2005:397-20.

[32] Yan L. ggvenn: Draw Venn Diagram by 'ggplot2' [R package]. R package version 0.1.10. 2023 Mar 31. [Accessed 2025 Sep 30]. Available from: https://CRAN.R-project.org/package=ggvenn.

[33] Kanehisa M. Toward understanding the origin and evolution of cellular organisms. Protein Sci. 2019 Nov;28(11):1947-51. [**PMID**: 31441146]

[34] Jain A, Tuteja G. TissueEnrich: Tissue-specific gene enrichment analysis. Bioinformatics. 2019 Jun 1;35(11):1966-67. [**PMID**: 30346488]

[35] GTEx Consortium. The GTEx Consortium atlas of genetic regulatory effects across human tissues. Science. 2020 Sep 11;369(6509):1318-30. [**PMID**: 32913098]

[36] Yu G, Wang LG, Han Y, He QY. clusterProfiler: an R package for comparing biological themes among gene clusters. OMICS. 2012 May;16(5):284-87. [**PMID**: 22455463]

[37] Yu G. Thirteen years of clusterProfiler. Innovation (Camb). 2024 Oct 21;5(6):100722. [**PMID**: 39529960]

[38] Szklarczyk D, Kirsch R, Koutrouli M, Nastou K, Mehryary F, Hachilif R, Gable AL, Fang T, Doncheva NT, Pyysalo S, Bork P, Jensen LJ, von Mering C. The STRING database in 2023: protein-protein association networks and functional enrichment analyses for any sequenced genome of interest. Nucleic Acids Res. 2023 Jan 6;51(D1):D638-46. [**PMID**: 36370105]

[39] Szklarczyk D, Gable AL, Nastou KC, Lyon D, Kirsch R, Pyysalo S, Doncheva NT, Legeay M, Fang T, Bork P, Jensen LJ, von Mering C. The STRING database in 2021: customizable protein-protein networks, and functional characterization of user-uploaded gene/measurement sets. Nucleic Acids Res. 2021 Jan 8;49(D1):D605-D612. Erratum in: Nucleic Acids Res. 2021 Oct 11;49(18):10800. [**PMID**: 33237311]

[40] Shannon P, Markiel A, Ozier O, Baliga NS, Wang JT, Ramage D, Amin N, Schwikowski B, Ideker T. Cytoscape: a software environment for integrated models of biomolecular interaction networks. Genome Res. 2003 Nov;13(11):2498-504. [**PMID**: 14597658]

[41] Bader GD, Hogue CW. An automated method for finding molecular complexes in large protein interaction networks. BMC Bioinformatics. 2003 Jan 13;4:2. [**PMID**: 12525261]

[42] Chin CH, Chen SH, Wu HH, Ho CW, Ko MT, Lin CY. cytoHubba: identifying hub objects and sub-networks from complex interactome. BMC Syst Biol. 2014;8 Suppl 4(Suppl 4):S11. [**PMID**: 25521941]

[43] Information NCfB. Description of SPRR1A (small proline rich protein 1A). [Internet]. National Center for Biotechnology Information; 2025. Accessed 5 July 2025. Available from: https://www.ncbi.nlm.nih.gov/gene?Cmd=DetailsSearch&Term=6698

[44] Schlingemann J, Hess J, Wrobel G, Breitenbach U, Gebhardt C, Steinlein P, Kramer H, Fürstenberger G, Hahn M, Angel P, Lichter P. Profile of gene expression induced by the tumour promotor TPA in murine epithelial cells. Int J Cancer. 2003 May 10;104(6):699-708. [**PMID**: 12640676]

[45] Sheng Z, Han W, Huang B, Shen G. Screening and identification of potential prognostic biomarkers in metastatic skin cutaneous melanoma by bioinformatics analysis. J Cell Mol Med. 2020 Oct;24(19):11613-18. [**PMID**: 32869947]

[46] Heikinheimo K, Kurppa KJ, Laiho A, Peltonen S, Berdal A, Bouattour A, Ruhin B, Catón J, Thesleff I, Leivo I, Morgan PR. Early dental epithelial transcription factors distinguish ameloblastoma from keratocystic odontogenic tumor. J Dent Res. 2015 Jan;94(1):101-11. [**PMID**: 25398365]

[47] Li J, Tang LL, Ma J. Survival-related indicators ALOX12B and SPRR1A are associated with DNA damage repair and tumor microenvironment status in HPV 16-negative head and neck squamous cell carcinoma patients. BMC Cancer. 2022 Jun 29;22(1):714. Erratum in: BMC Cancer. 2022 Jul 11;22(1):755. [**PMID**: 35768785]

[48] Database GC. Description of S100A2 (S100 Calcium Binding Protein A2). [Internet]. GeneCards; 2025. Accessed 13 July 2025. Available from: https://www.genecards.org/cgi-bin/carddisp.pl?gene=S100A2

[49] van Dieck J, Teufel DP, Jaulent AM, Fernandez-Fernandez MR, Rutherford TJ, Wyslouch-Cieszynska A, Fersht AR. Posttranslational modifications affect the interaction of S100 proteins with tumor suppressor p53. J Mol Biol. 2009 Dec 18;394(5):922-30. [**PMID**: 19819244]

[50] Mueller A, Schäfer BW, Ferrari S, Weibel M, Makek M, Höchli M, Heizmann CW. The calcium-binding protein S100A2 interacts with p53 and modulates its transcriptional activity. J Biol Chem. 2005 Aug 12;280(32):29186-93. [**PMID**: 15941720]

[51] Samarasinghe V, Madan V. Nonmelanoma skin cancer. J Cutan Aesthet Surg. 2012 Jan;5(1):3-10. [**PMID**: 22557848]

[52] Gene Ontology Consortium. Immune response-activating cell surface receptor signaling pathway (GO:0002429). [Internet]. Gene Ontology Resource; 2025. Accessed 30 Sept 2025. Available from: http://amigo.geneontology.org/amigo/term/GO:0002429

[53] Consortium GO. Immune response-regulating cell surface receptor signaling pathway (GO:0002768). [Internet]. Gene Ontology Resource; 2025. Accessed 30 Sept 2025. Available from: http://amigo.geneontology.org/amigo/term/GO:0002768

[54] Kayagaki N, Kornfeld OS, Lee BL, Stowe IB, O'Rourke K, Li Q, Sandoval W, Yan D, Kang J, Xu M, Zhang J, Lee WP, McKenzie BS, Ulas G, Payandeh J, Roose-Girma M, Modrusan Z, Reja R, Sagolla M, Webster JD, Cho V, Andrews TD, Morris LX, Miosge LA, Goodnow CC, Bertram EM, Dixit VM. NINJ1 mediates plasma membrane rupture during lytic cell death. Nature. 2021 Mar;591(7848):131-36. [**PMID**: 33472215]

[55] Kurosaki T, Tsukada S. BLNK: connecting Syk and Btk to calcium signals. Immunity. 2000 Jan;12(1):1-5. [**PMID**: 10661400]

[56] Romano V, Belviso I, Venuta A, Ruocco MR, Masone S, Aliotta F, Fiume G, Montagnani S, Avagliano A, Arcucci A. Influence of Tumor Microenvironment and Fibroblast Population Plasticity on Melanoma Growth, Therapy Resistance and Immunoescape. Int J Mol Sci. 2021 May 17;22(10):5283. [**PMID**: 34067929]

[57] Michaelis UR. Mechanisms of endothelial cell migration. Cell Mol Life Sci. 2014 Nov;71(21):4131-48. [**PMID**: 25038776]

[58] Liang Y, Min D, Fan H, Liu K, Tu J, He X, Liu B, Zhou L, Liu S, Sun X. Discovery of a first-in-class ANXA3 degrader for the treatment of triple-negative breast cancer. Acta Pharm Sin B. 2023 Apr;13(4):1686-98. [**PMID**: 37139408]

[59] Lacina L, Plzak J, Kodet O, Szabo P, Chovanec M, Dvorankova B, Smetana K Jr. Cancer Microenvironment: What Can We Learn from the Stem Cell Niche. Int J Mol Sci. 2015 Oct 12;16(10):24094-110. [**PMID**: 26473842]

[60] Farsam V, Basu A, Gatzka M, Treiber N, Schneider LA, Mulaw MA, Lucas T, Kochanek S, Dummer R, Levesque MP, Wlaschek M, Scharffetter-Kochanek K. Senescent fibroblast-derived Chemerin promotes squamous cell carcinoma migration. Oncotarget. 2016 Dec 13;7(50):83554-69. [**PMID**: 27907906]

[61] Information NCfB. MYLK myosin light chain kinase [Homo sapiens (human)] (Gene ID: 4638). [Internet]. National Center for Biotechnology Information; updated 27 Sep 2025. Accessed 27 Mar 2025. Available from: https://www.ncbi.nlm.nih.gov/gene/4638.

[62] Information NCfB. ACTN1 actinin alpha 1 [Homo sapiens (human)] (Gene ID: 87). [Internet]. National Center for Biotechnology Information; updated 14 Sep 2025. Accessed 27 Mar 2025. Available from: https://www.ncbi.nlm.nih.gov/gene/87.

[63] D'Arino A, Caputo S, Eibenschutz L, Piemonte P, Buccini P, Frascione P, Bellei B. Skin Cancer Microenvironment: What We Can Learn from Skin Aging? Int J Mol Sci. 2023 Sep 13;24(18):14043. [**PMID**: 37762344]

[64] Information NCfB. PHKA1 phosphorylase kinase regulatory subunit alpha 1 [Homo sapiens (human)] (Gene ID: 5255). [Internet]. National Center for Biotechnology Information; updated 9 Sep 2025. Available from: https://www.ncbi.nlm.nih.gov/gene/5255.

[65] Liu S, Liu S, Wang X, Zhou J, Cao Y, Wang F, Duan E. The PI3K-Akt pathway inhibits senescence and promotes self-renewal of human skin-derived precursors in vitro. Aging Cell. 2011 Aug;10(4):661-74. [**PMID**: 21418510]

[66] Teng Y, Fan Y, Ma J, Lu W, Liu N, Chen Y, Pan W, Tao X. The PI3K/Akt Pathway: Emerging Roles in

Skin Homeostasis and a Group of Non-Malignant Skin Disorders. Cells. 2021 May 17;10(5):1219. [**PMID**: 34067630]

[67] Information NCfB. RAC3 Rac family small GTPase 3 [Homo sapiens (human)] (Gene ID: 5881). [Internet]. National Center for Biotechnology Information; updated 27 Sep 2025. Available from: https://www.ncbi.nlm.nih.gov/gene/5881.

[68] Gene Ontology Consortium. Peptide cross-linking (GO:0018149). [Internet]. Gene Ontology Resource; 2025. Accessed 25 Mar 2025. Available from: http://amigo.geneontology.org/amigo/term/GO:0018149.

[69] Pande P, Ji S, Mukherjee S, Schärer OD, Tretyakova NY, Basu AK. Mutagenicity of a Model DNA-Peptide Cross-Link in Human Cells: Roles of Translesion Synthesis DNA Polymerases. Chem Res Toxicol. 2017 Feb 20;30(2):669-77. [**PMID**: 27951635]

[70] Kuehne A, Hildebrand J, Soehle J, Wenck H, Terstegen L, Gallinat S, Knott A, Winnefeld M, Zamboni N. An integrative metabolomics and transcriptomics study to identify metabolic alterations in aged skin of humans in vivo. BMC Genomics. 2017 Feb 15;18(1):169. [**PMID**: 28201987]

[71] Padilla RS, Sebastian S, Jiang Z, Nindl I, Larson R. Gene expression patterns of normal human skin, actinic keratosis, and squamous cell carcinoma: a spectrum of disease progression. Arch Dermatol. 2010 Mar;146(3):288-93. [**PMID**: 20231500]

[72] Talantov D, Mazumder A, Yu JX, Briggs T, Jiang Y, Backus J, Atkins D, Wang Y. Novel genes associated with malignant melanoma but not benign melanocytic lesions. Clin Cancer Res. 2005 Oct 15;11(20):7234-42. [**PMID**: 16243793]